Asteroids, Comets, Meteors
Proceedings IAU Symposium No. 229, 2005
D. Lazzaro, S. Ferraz-Mello & J.A. Fernánez, eds.

doi:10.1017/S1743921305006708

Review of Spitzer Space Telescope observations of small bodies

Y. R. Fernández[1], J. P. Emery[2], D. P. Cruikshank[2] and J. A. Stansberry[3]

[1]Dept. of Physics, Univ. of Central Florida, 4000 Central Florida Blvd., Orlando, FL 32816-2385 U.S.A.; Formerly at Institute for Astronomy, University of Hawai'i at Mānoa, 2680 Woodlawn Drive, Honolulu, HI 96822 U.S.A.
email: yan@physics.ucf.edu

[2]NASA Ames Research Center, MS 245-6, Moffett Field, CA 94035 U.S.A.
email: jemery@mail.arc.nasa.gov, Dale.P.Cruikshank@nasa.gov

[3]Steward Observatory, University of Arizona 933 N. Cherry Avenue, Tucson, AZ 85721 U.S.A.
email: stansber@as.arizona.edu

Abstract. The *Spitzer Space Telescope* (SST), aloft for over two years at time of writing, has so far devoted almost 600 hours of observing time to Solar System science, and small bodies make up a significant fraction of the objects that have been observed. For the first time we now have high accuracy mid-infrared data to study the fundamental mineralogical and physical properties of a large number of objects of different types. In this paper we review some of the exciting recent results derived from SST photometry (in six bands from 3.6 to 70 μm) and spectroscopy (from 5 to 40 μm) of asteroids and comets. The observations reveal their spectral energy distributions (SEDs), and we discuss three important science goals that can be addressed with these data: (1) finding compositional diagnostics of these objects, (2) determining their bulk thermal properties, and (3) understanding the surface evolution of primitive and icy bodies. We focus primarily on comet-asteroid transition objects, low-albedo asteroids, cometary nuclei, Trojans, Centaurs, and trans-Neptunian objects. In particular, we will show: emissivity features in the SEDs and identification of the compositional sources, the constraints on thermal inertia and infrared beaming through the samples of the thermal continuum, and an intercomparison of albedos across dynamically-related bodies.

Keywords. comets: general, infrared: solar system, minor planets

1. Introduction

The *Spitzer Space Telescope* (SST) was launched on 2003 August 25 as the fourth of NASA's "Great Observatories," covering the mid- to far-infrared wavelength regime. A review of the spacecraft design and instrument complement is given by Werner, Roellig, Low, *et al.* (2004). The spacecraft is in a heliocentric orbit that takes it farther and farther from Earth over the course of its expected five to six-year lifespan. The telescope itself, with a 0.85-m diameter primary mirror, is cooled to cryogenic temperatures and for the most part is thermally isolated from the rest of the spacecraft. The combination of innovative design and orbit reduces the heat environment surrounding the instruments, and so gives them spectacular infrared sensitivity in comparison to previous infrared space telescopes.

There are three infrared science instruments: InfraRed Array Camera (IRAC), InfraRed Spectrograph (IRS), and Multiband Imaging Photometry for *Spitzer* (MIPS). All three instruments have imaging capability, and two (IRS and MIPS) have spectroscopic

modes. IRAC (Fazio, Hora, Allen, *et al.* 2004) obtains broadband images at four wavelengths $\lambda = 3.6$, 4.5, 5.8, and 8.0 μm. Each wavelength has its own detector with a $(5.2')^2$ field of view. The imaging mode for MIPS (Rieke, Young, Engelbracht, *et al.* 2004) is similar, with three wavelengths – 24, 70, and 160 μm – each having its own detector. The fields of view are $(5.4')^2$, 5.3′-by-2.6′, and 5.3′-by-0.5′, respectively. Finally, IRS (Houck, Rellig, van Cleve, *et al.* 2004) can perform small field of view (about $1'^2$) imaging at $\lambda = 16$ and 22 μm; this is primarily intended for peak-up imaging to place a target within an IRS slit.

MIPS also has a spectroscopic mode, where a slit spectrum of low resolution ($R \approx 15$ to 25) can be obtained over $\lambda = 60$ to 100 μm. However, the primary spectroscopic instrument is IRS with four modules that cover $\lambda = 5.2$ to 38 μm. Two modules work at low resolution ($R \approx 100$) and two at high ($R \approx 600$). Each module has its own single slit.

2. Observations

2.1. *Telescope Activity*

In practice, observing with SST occurs through scripts that are created by the observer using a software tool ("SPOT") provided by the Spitzer Science Center. A script for a single independently-schedulable observation automatically calculates telescope and instrument overheads, and the duration of the observation includes these overheads.

Counting all observations through 2005 October 5, which includes all of General Observer Cycle 1 and the start of Cycle 2, there have been 10,990 hours' worth of scripts observed. Of those, 3095 hours were for the six Legacy projects, which are virtually complete. Of the remaining 7895 hours, 592 hours (about 7.5%) have been devoted to Solar System science. This fraction of time is completely consistent with the proposal submission fraction from the Solar System community. Including Cycle 2 (which started in June) and including Director's Discretionary Time, there are currently 58 *Spitzer* projects directly related to our Solar System.

Almost three-fourths of the telescope time for Solar System observations has employed MIPS, and most of the rest is IRS. IRAC currently accounts for under 4% of the time. (Note that one cannot observe with multiple instruments simultaneously.) Among non-Solar System programs, IRAC was the most-used instrument (in terms of hours) for the Legacy projects, and has been used for over one-fourth of the other non-Solar System telescope time. The relatively small use of IRAC for Solar System science is partly due to the shape of the spectral energy distributions (SEDs) of many objects; the emission reaches a local minimum where the reflected and thermal components cross, and this often occurs within the IRAC wavelengths. Nonetheless, IRAC is a sensitive instrument and several planetary science programs are making use of it.

2.2. *Imaging and Photometry*

Figure 1 displays what minimum requirements are needed to obtain useful IRAC data in a relatively short amount of observing time. For an object with a geometric albedo of 0.10 and a given heliocentric distance r, we have plotted the requisite effective radius and requisite R-band magnitude necessary to obtain a 4-σ detection of the object in each IRAC band in 1080 seconds of integration. Such an observation would take 50 minutes. The sensitivities of the four IRAC bands (in increasing wavelength) are 0.42, 0.68, 4.5, and 5.3 μJy, respectively, for these integration times. This assumes a "high" background appropriate for the ecliptic. Note that in practice it is possible to achieve

https://doi.org/10.1017/S1743921305006708 Published online by Cambridge University Press

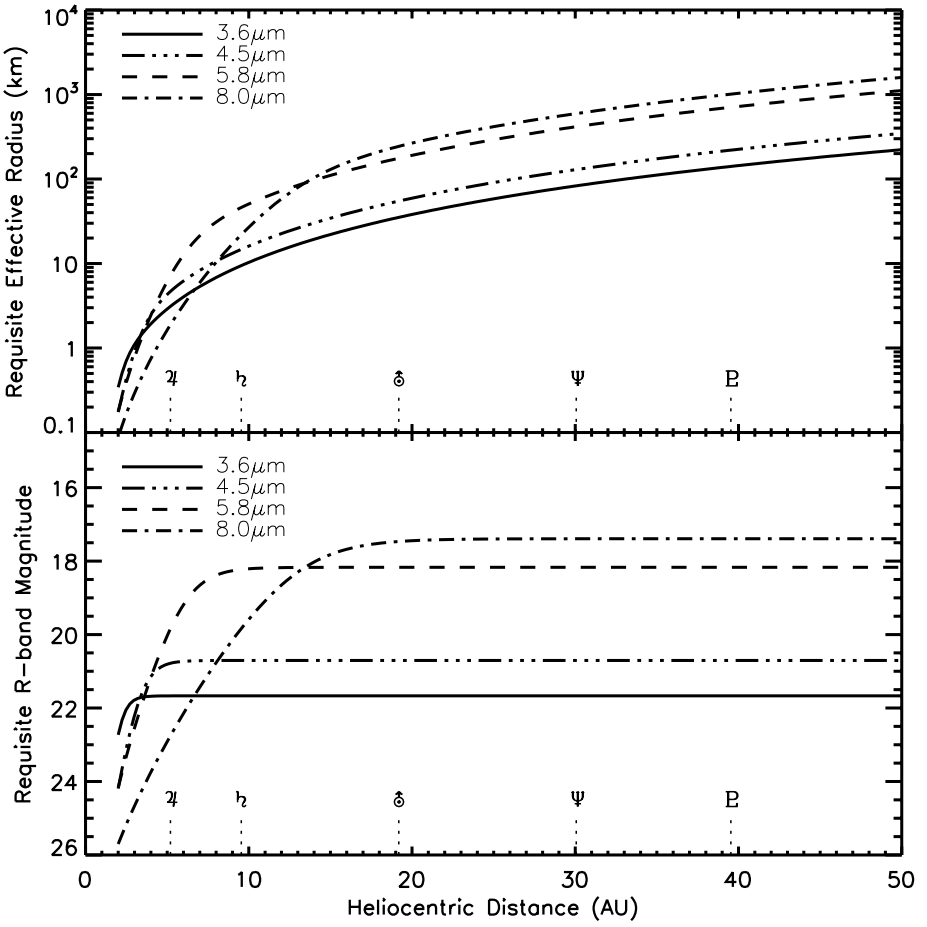

Figure 1. Minimum radius (top) and maximum magnitude (bottom) required to obtain $S/N = 4$ in a given IRAC band for a given heliocentric distance after 1080 seconds of integration. Calculations assume a geometric albedo of 0.10, phase slope parameter of 0.05, solar colors, and an observation occuring at quadrature. Semimajor axes of major planets and Pluto are marked.

sensitivities below the so-called "confusion limit" by obtaining shadow observations, a technique uniquely available to Solar System projects.

One obvious feature in Fig. 1 is the flattening out of the magnitude above a certain distance. This shows at which r the flux at a wavelength is dominated by reflected sunlight and not thermal emission.

We show an analogous graph for MIPS in Fig. 2, where we have assumed 2800 seconds of integration at 24 μm, 600 seconds at 70 μm, and 120 seconds at 160 μm. If all in one observing script, such an observation would take about 115 minutes. The sensitivities of the three MIPS bands (in increasing wavelength) are 0.021, 2.3, and 35.0 mJy, respectively, for these integration times (and a "high" background). As with IRAC, shadowing of MIPS observations can also be used to reach deeper sensitivites. Note that in many Solar System projects, observations at 160 μm are difficult. For objects emitting according to the Rayleigh-Jeans law in the 70 to 160 μm region, the relative sensitivities are such that the S/N at 160 μm will be a factor of about 35 smaller than that at 70 μm for the same exposure time.

https://doi.org/10.1017/S1743921305006708 Published online by Cambridge University Press

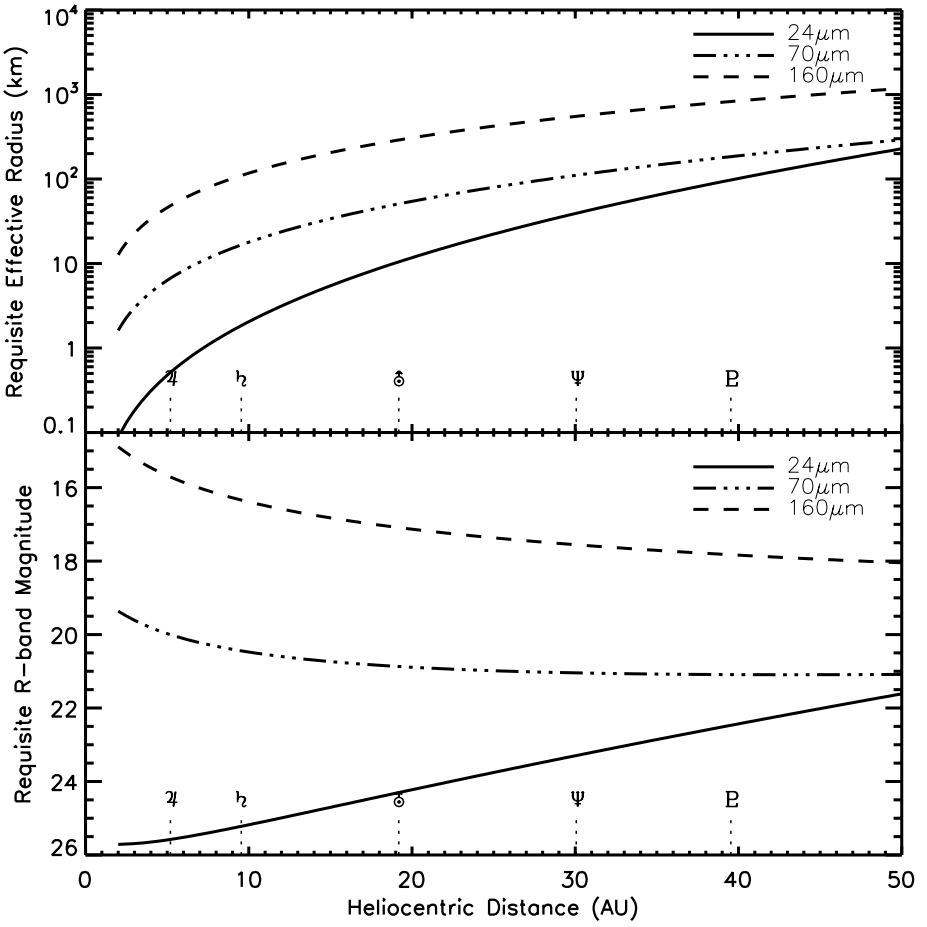

Figure 2. Minimum radius (top) and maximum magnitude (bottom) required to obtain $S/N = 4$ in a given MIPS band for a given heliocentric distance. Exposure times of 2800, 600, and 120 seconds were assumed for the three bands. Calculations assume a geometric albedo of 0.10, phase slope parameter of 0.05, solar colors, and an observation occuring at quadrature. Semimajor axes of major planets and Pluto are marked.

The figure demonstrates that for most Solar System objects, 24 μm is the better choice for obtaining a simple detection. While one could observe longer at 70 μm to bring the crossing point of the 24 μm and 70 μm curves in Fig. 2 to smaller r, it turns out that there is much more overhead for 70 and 160 μm observing.

3. Results and Discussion

3.1. *Topics*

A report on "small bodies" could encompass many types of Solar System objects. SST has already observed many small regular and irregular satellites, comets, near-Earth asteroids, unusual asteroids, small Main-Belt asteroids, zodiacal dust, and Trojans†.

† A list of all projects as well as information on Solar System observing is maintained by one of us (YRF) at URL `http://www.physics.ucf.edu/~yfernandez/sss.html`.

https://doi.org/10.1017/S1743921305006708 Published online by Cambridge University Press

There are a few projects that we will not discuss here: projects devoted to the outer planets; projects focussing on Pluto and the other, very large TNOs; and projects in Cycle 2 that have yet to receive any observations. This leaves a core group of about 12 projects devoted to dust and 15 projects devoted to the solid bodies themselves. The results of some of these projects will be discussed in the following subsections.

3.2. *Dust*

There are over twenty projects devoted to Solar System dust – more than one-third of all planetary programs. In particular there are two "medium" projects (i.e. allocation between 50 and 200 hours), run by M. V. Sykes (in Cycle 1) and W. F. Bottke (in Cycle 2), studying the asteroidal dust bands. The combined allocation of these projects is about 270 hours, so they will provide much deeper and more extensive maps of the bands' surface brightness than were possible before. Also of note is a multi-cycle project run by S. Jayaraman to map the spatial extent of the dust cloud in Earth's orbital wake. This is a fascinating and clever application of Spitzer's unique position on an independent heliocentric orbit. During Cycle 2, Spitzer will be from 0.19 to 0.32 AU from Earth, giving us an unprecedented vantage point on the near-Earth dust environment. All of these projects are still in the early stages of analysis.

Reach (2004) and collaborators are doing an extensive survey of the dynamics of cometary dust trails. While trails have been seen in several comets with IRAS (Sykes & Walker 1992) and from ground-based data (Ishiguro, *et al.* 2003), only Spitzer has allowed us to determine the true frequency of their occurrence. Reach (2004) finds that a large fraction of all Jupiter-family comets have trails. Further analysis will reveal if the emission of very large dust grains is correlated with the gas production rate or the orbital anomaly.

Woodward, Kelley, Harker, *et al.* (2005) have several projects devoted to understanding composition of cometary dust in both Jupiter-family and long-period Oort-Cloud comets. Ground-based mid-IR spectroscopy in the 8 to 13 μm region has in the past given us insight into basic silicate composition of dust. However, this technique can only be used on relatively few comets for lack of sufficient signal-to-noise. Spitzer on the other hand has much better sensitivity limitations and a comprehensive survey of comets from all dynamical classes is now possible. Since comets were formed throughout the outer-planet region in the protoplanetary disk, there may be a signature of a compositional gradient within the comets of differing dynamical classes.

Finally, one of the most exciting dust-related projects involves observations of comet Tempel 1. In July 2005, the Discovery-class spacecraft *Deep Impact* delivered a 10-km/s impactor onto the surface of this comet (A'Hearn, Belton, Delamere, *et al.* 2005). Spitzer's IRS observed the exact moment of impact, taking 5.2–8.7 μm spectra with high temporal frequency to watch the rapidly changing post-impact environment (van Cleve, Lisse, Grillmair, *et al.* 2005). Spectra through all of IRS's range were also obtained in the hours following impact. The data are particularly rich in showing emission from a wide variety of compounds in the impact ejecta. Again, analysis is very preliminary, but since there is a good chance that Spitzer was observing relatively unprocessed subsurface material, the data hold great promise for understanding what pristine material comets hold.

3.3. *Asteroid Counts*

One project performed early in the mission was the Ecliptic Plane Survey (EPS), as discussed by Meadows, Bhattacharya, Reach, *et al.* (2004). The goal was to characterize the sky-plane density of small (kilometer-sized) Main Belt (MB) asteroids, which is helpful for understanding not only the size distribution in the MB but also the contamination

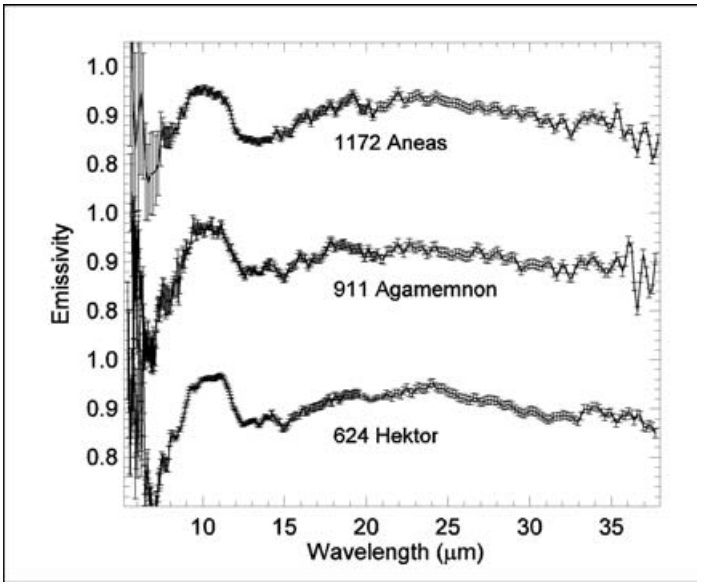

Figure 3. Emissivity plot of three Trojans, from work by Emery, Cruikshank, & van Cleve (2006) using the IRS on SST. Each object's SED has been divided by the continuum as determined using the standard thermal model for slow-rotators (Lebofsky & Spencer 1989).

rate by asteroids in sidereally-tracked fields. Our understanding of these small MB objects is very incomplete. The EPS mapped two fields with IRAC at 8 μm and MIPS at 24 μm, with the fields at two ecliptic latitudes, 0° and +5°. Most of the asteroids that were found were previously unknown even though the exposures were relatively short, demonstrating that Spitzer is a highly efficient asteroid finder. Meadows, Bhattacharya, Reach, *et al.* (2004) report that the ratio of objects found at the two latitudes is nominally higher than expected, although it is not clear yet whether this difference is statistically significant. Poisson statistics of the EPS's asteroid counts coupled with the spread in the predictive models indicate that further observations are necessary at a variety of ecliptic latitudes. Spitzer has given us new clues to solve a problem that was quite infeasible before, and even a modest investment in Spitzer time would yield significant advances in our knowledge of the small end of the asteroid distribution.

3.4. *Composition*

The technique of measuring an object's SED with IRS is a powerful way to find spectral diagnostics that reveal clues to the object's composition. Emery, Cruikshank, & van Cleve (2006) give a detailed analysis of the spectra of three Jovian Trojan asteroids, (624) Hektor, (911) Agamemnon, and (1172) Aneas. As the Trojans are uniquely placed in the Solar System one primary motivation for this study is to understand their constituents in the context of comets and outer Solar System asteroids, and in particular the organic component and the specific proportions of silicates.

The emissivity spectra of the three Trojans are shown in Fig. 3, and spectral structure is clearly evident in all of them. Emery, Cruikshank, & van Cleve (2006) point out the following features: An emission plateau at about 9.1 to 11.5 μm has a spectral contrast of 10 to 15%, and a broader emission high is apparent from about 18 to 28 μm. More subtle features include a possible double peak within the 18 to 28 μm rise and another rise near 34 μm. Differences among the Trojan spectra are also subtle. Hektor and Agamemnon exhibit a small (few % contrast) feature near 14 μm that is absent from the Aneas

https://doi.org/10.1017/S1743921305006708 Published online by Cambridge University Press

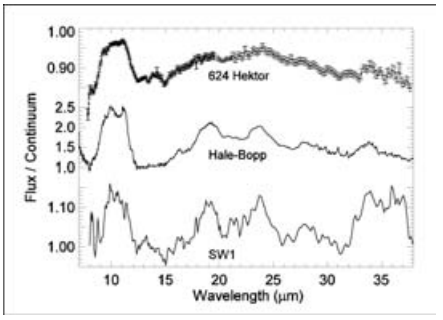

Figure 4. Comparison of the emissivity between a Trojan, Hektor, and two comets, C/1995 O1 Hale-Bopp, and 29P/Schwassmann-Wachmann 1. The figure is taken from the work by Emery, Cruikshank, & van Cleve (2006). Cometary data from Crovisier, Leech, Bockelee-Morvan, *et al.* (1997) and Stansberry, van Cleve, Reach, *et al.* (2004).

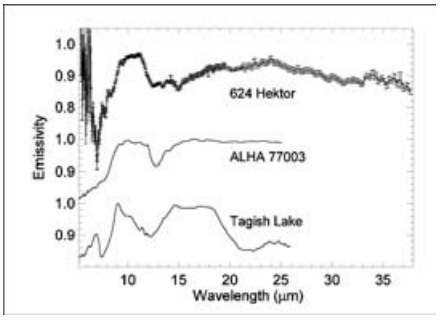

Figure 5. Comparison of the emissivity between a Trojan, Hektor, and two meteorites, the CO3-type ALH 77003 and Tagish Lake. The figure is taken from the work by Emery, Cruikshank, & van Cleve (2006).

spectrum. Hektor's 10-μm plateau is slightly tilted, with a peak at about 11.2 μm, whereas those of Agamemnon and Aneas are relatively flat and perhaps even a bit rounded.

Note that care must be taken near wavelengths where spectra from two different orders have been joined. This occurs over the 14.0-to-14.5 μm interval and the 19.5-to-21.3 μm interval. However Emery, Cruikshank, & van Cleve (2006) state that the 14-μm feature in Fig. 3 is likely real, and that the 20.5-μm local minimum is broader than would be expected if it were due to poor order stitching.

It is interesting to compare these spectra with that of cometary dust, meteorites, and laboratory analogues. This is shown in Figs. 4 and 5. The overall similarities with both a long-period comet (Hale-Bopp) and a short-period comet/active Centaur (P/Schwass\-mann-Wachmann 1) are striking. The grains on the surface of Hektor, though making up a solid body, have a similar SED to the micron-sized grains in these comets' comae. Hektor's surface has fine-grained silicates, and when Emery, Cruikshank, & van Cleve (2006) compare the specific band positions with comet spectra, the conclude that Hektor's is dominated by a Mg-rich, amorphous silicate mineralogy (though they also state that the analysis is hampered by limitations of spectral libraries and scattering theories for the appropriate wavelengths).

In Fig. 5, the closest meteorite match that Emery, Cruikshank, & van Cleve (2006) found was with ALH 77003, a CO3 meteorite. Interestingly, it appears that the spectral characteristics of Tagish Lake meteorite are very unlike that of Hektor. The fact that Tagish Lake is thought to be an analog to the D-type asteroids – of which Hektor is a member – apparently does not imply that the mid-IR spectrum is similar (although the thermal emission spectrum for Tagish Lake is still somewhat uncertain).

The presence of fine-grained silicates in Hektor supports the view that the visible/near-IR spectral characteristics (low albedo, red slope, no absorption features) are due to silicates, not organics. The middle part of the Solar System, the transition region between rocky and icy objects, does not appear to contain an abundance of organic material. Emery, Cruikshank, & van Cleve (2006) suggest that the spectral (taxonomic) trends observed in the Main Belt are due to changes in silicate mineralogy with heliocentric distance. Rather than organics causing red spectral slopes in the outer Main Belt and Trojan

https://doi.org/10.1017/S1743921305006708 Published online by Cambridge University Press

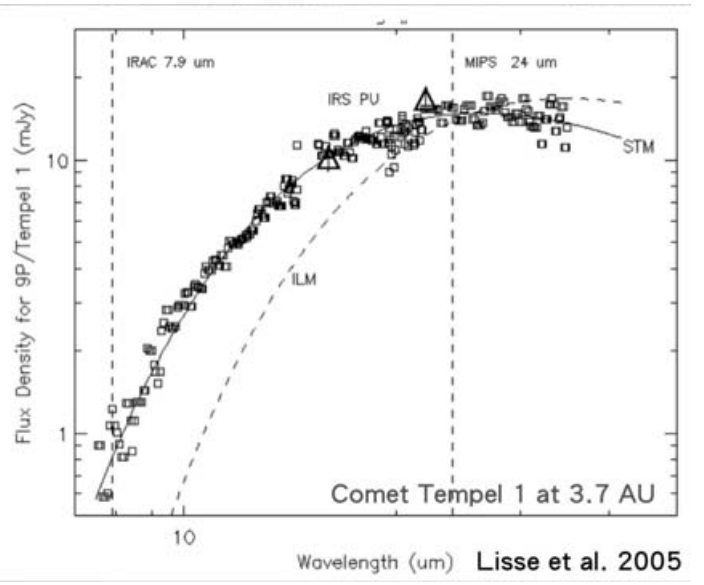

Figure 6. IRS spectrum (squares) of comet 9P/Tempel 1's nucleus when it was at 3.6 AU in March 2004 (Lisse, A'Hearn, Groussin, *et al.* 2005). The slow-rotator thermal model ("STM") fits very well; in contrast, the rapid-rotator model ("ILM") fails. Also plotted (triangles) is photometry from the IRS peak-up camera. Figure courtesy C. M. Lisse.

swarms, it is likely that these surfaces and their spectra are dominated by amorphous silicates. Similarities with comet spectra, and therefore silicate mineralogy, suggest that whereas the silicate fraction in the inner Solar System varies significantly in mineralogy due largely to a temperature gradient during and after accretion, the middle and outer nebular silicate mineralogy may have been more homogenous. Mid-IR spectral observations of a much larger sample of asteroids and comets (as made possible by Spitzer) that span a range of taxonomic types, particularly those without diagnostic absorptions in the visible/near-IR, will test these ideas and provide more insight into silicate mineralogy in the Solar System.

3.5. *Thermal Properties*

One significant mission-oriented result from SST involves comet 9P/Tempel 1. Observations in March 2004 using IRS spectroscopy and imaging allowed once and for all the effective radius (over a rotation period) and the geometric albedo of the nucleus to be pinned down. This was accomplished well before the arrival of the *Deep Impact* spacecraft; understanding the basic physical properties of the nucleus beforehand was crucial for the mission success, in particular for the design and planning of the impactor's autonomous targeting software. The analysis, which showed an effective radius of 3.3 ± 0.2 km and a visible-wavelength geometric albedo of 0.04 ± 0.01, is reported by Lisse, A'Hearn, Groussin, *et al.* (2005). The good signal-to-noise ratio of the spectrum allowed these workers to also constrain the thermal inertia, as shown in Fig. 6. In the past thermal inertia – and hence the applicability of the slow-rotator thermal model (Lebofsky & Spencer 1989) – has been very difficult to quantify in cometary nuclei, since in the large majority of cases ground-based observing yields only broadband photometry at modest S/N. The SST observations confirmed that Tempel 1's thermal inertia was very low, less than that of the Moon, giving confidence that the standard thermal

https://doi.org/10.1017/S1743921305006708 Published online by Cambridge University Press

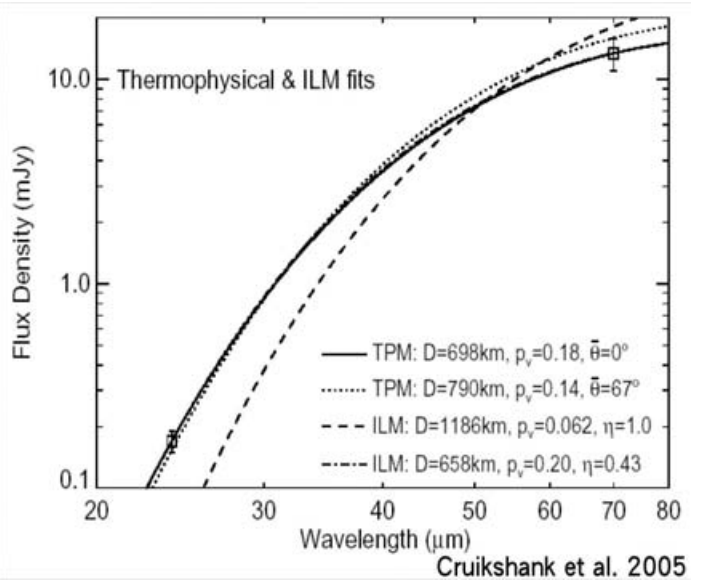

Figure 7. Photometry of TNO 2002 AW_{197} from MIPS at 24 and 70 μm (squares). Various thermal models are plotted as well. The best fitting model is one that is intermediate between the slow- and rapid-rotator models, and that requires some appreciable obliquity of the rotation axis. The visible-wavelength magnitudes are well constrained, and a geometric albedo of about 0.15 was derived.

model for slow rotators is valid. And indeed, the conversion of radiometry to nucleus size was confirmed by the *Deep Impact* flyby, which encountered a nucleus of effective radius 3.0 ± 0.1 km (A'Hearn, Belton, Delamere, *et al.* 2005).

3.6. *Albedo Diversity*

Arguably one of the most significant Solar System results to come out of SST observations is the diversity of albedos among the Centaur and TNO populations. This was tentatively suspected from some earlier low-S/N ground-based thermal measurements (e.g. Fernández, Jewitt, & Sheppard 2002). However the SST results are far superior.

Two projects, whose PIs are G. Rieke and D. P. Cruikshank, have been surveying several of these objects at 24 and 70 μm with MIPS in order to constrain their thermal properties, radii, and albedos. The results have been described at conferences by Stansberry, Cruikshank, Grundy, *et al.* (2005)† and Cruikshank, Barucci, Emery, *et al.* (2005). A paper by J. A. Stansberry is in preparation.

A figure from the work by Cruikshank, Stansberry, Emery, *et al.* (2005) on 2002 AW_{197}, one of the first TNOs to be observed by SST, is shown in Fig. 7. The analysis comes down to finding what thermal model matches the observed 24-to-70 μm color. In this case, and in virtually all objects at these heliocentric distances, neither the slow-rotator (STM) nor the rapid-rotator (ILM) models is adequate. The STM can be made to fit if the so-called "beaming parameter" is set to 1.2. This is not an unphysical number, but it does indicate that there is some thermal emission from the night side of the object. Therefore to achieve a more robust calculation of the effective radius, an intermediate thermal model is required. Cruikshank, Stansberry, Emery, *et al.* (2005) use a thermophysical model

† Note that a few of the albedos provided in the published abstract were updated in the oral presentation itself.

https://doi.org/10.1017/S1743921305006708 Published online by Cambridge University Press

(TPM) that accounts for night-side emission and for the obliquity of the rotation axis with respect to the Sun-Earth-object plane. For 2002 AW_{197}, an appreciable obliquity was required to achieve the best fit to the MIPS color. In combination with the already-known visible magnitude, Cruikshank, Stansberry, Emery, *et al.* (2005) derive a geometric albedo of 0.15, much higher than the 0.04 canonically assumed in the pre-Spitzer era.

The analysis of 7 TNOs and 7 Centaurs by Stansberry, Cruikshank, Grundy, *et al.* (2005) and Cruikshank, Barucci, Emery, *et al.* (2005) continues the trend. The TNOs and Centaurs have a wide distribution of albedos, with the TNOs ranging from about 0.01 to 0.2, and the Centaurs ranging from about 0.02 to 0.07. Chiron's albedo is already known to be about 0.12 (Campins, Telesco, Osip, *et al.* 1994, Fernández, Jewitt, & Sheppard 2002), extending the Centaurs' range, but so far the Centaurs do not appear to be as reflective as some TNOs. Furthermore there is as yet no correlation observed between the albedo and the radius or the albedo and the V-R color. The observations are continuing however and it is expected that at the end of the project useful radius and albedo results will have been derived for 20 TNOs and 12 Centaurs.

One implication of the wide range of albedos is the connection between surface albedo and cometary activity. Several Centaurs are actively outgassing, and it would be interesting to see if there is a correlation between albedo and activity. Do the active Centaurs all have high albedos? Do Centaurs that have been only recently deactivated have high or low albedos? How long does it take for surface volatiles to disappear? Is albedo correlated with dynamical age? How long would a Centaur need to stay near ∼5 to 6 AU before its albedo would drop to the 0.04 to 0.05 that is the average of cometary nuclei and Trojans? Our understanding of the Centaur albedos can give clues to some fundamental problems of cometary evolution.

Lastly, we mention one special object in the sample: 1999 TC_{36}, a binary TNO. Measurements of the thermal emission have constrained the radii and thus the volume of the two objects. The masses have been constrained from the orbit, and so Stansberry *et al.* (2006) have calculated a bulk density of 0.3 to 0.9 g/cm^3. This implies that the object would be very porous, with a porosity of at least 50%. While this would require a large amount of void space, the number is not too much higher than the porosity calculated by Jewitt & Sheppard (2002) for the TNO (50000) Varuna.

4. Summary

We have given a brief review of Solar System observations made by the Spitzer Space Telescope since its launch in August 2003. At time of writing, almost five dozen Solar System projects have been allocated time, and they are in various stages of completion. Analysis is still preliminary for many of these projects, and much of the data are still proprietary. The Solar System component has so far accounted for 7.5% of the total non-Legacy SST observing time.

We have also given a brief overview of some of the projects that are devoted to dust, asteroids, and comets. While far from complete, the review of these projects gives a flavor for the type of cutting edge Solar System science from SST.

Acknowledgements

YRF would like to acknowledge the support of a SIRTF Fellowship provided by the Spitzer Science Center and JPL. All the authors appreciate the help of the SSC in supporting the observations reported here, and of the PIs in making their early results available to a wide audience.

References

A'Hearn, M. F.,Belton, M. J. S.,Delamere, A., & Blume, W. H.2005, *Sp. Sci. Rev.* 117, 1

Campins, H.,Telesco, C. M.,Osip, D. J.,Rieke, G. H.,Rieke, M. J.,& Schulz, B.1994, *Astron. J.* 108, 2318

Crovisier, J.,Leech, K.,Bockelee-Morvan, D.,Brooke, T. Y.,Hanner, M. S.,Altieri, B.,Keller, H. U.,& Lellouch, E.1997, *Science* 275, 1904

Cruikshank, D. P.,Barucci, A.,Emery, J. P.,Fernández, Y.,Grundy, W.,Noll, K.,& Stansberry, J. A.2005, in: B.Reipurth, D.Jewitt& K.Keil (eds.), *Protostars and Planets V* (Tucson: U. Arizona), submitted

Cruikshank, D. P.,Stansberry, J. A.,Emery, J. P.,Fernández, Y.R.,Werner, M. W.,Trilling, D. E.,& Rieke, G. H.2005, *Astrophys. J.* 624, L53

Emery, J. P.,Cruikshank, D. P.,& van Cleve, J.2006, *Icarus*, submitted

Fazio, G. G., and 64 colleagues 2004, *Astrophys. J. Supp. Ser.* 154, 10

Fernández, Y. R.,Jewitt, D. C.,& Sheppard, S. S.2002, *Astron. J.* 123, 1050

Houck, J. R., and 34 colleagues 2004, *Astrophys. J. Supp. Ser.* 154, 18

Ishiguro, M.,Kwon, S. M.,Sarugaku, Y.,Hasegawa, S.,Usui, F.,Nishiura, S.,Nakada, Y.,& Yano, H.2003*Astrophys. J.* 589, L101

Jewitt, D. C.,& Sheppard, S. S.2002, *Astron. J.* 123, 2110

Lebofsky, L. A.,& Spencer, J. R.1989, in: R. P.Binzel, T.Gehrels, M. S.Matthews (eds.), *Asteroids II* (Tucson: U. Arizona), p. 128

Lisse, C. M.,A'Hearn, M. F.,Groussin, O.,Fernández, Y. R.,Belton, M. J. S.,van Cleve, J. E.,Charmandaris, V.,Meech, K. J.,& McGleam, C.2005, *Astrophys. J.* 625, L139

Meadows, V. S.,Bhattacharya, B.,Reach, W. T.,Grillmair, C.,Noriega-Crespo, A.,Ryan, E. L.,Tyler, S. R.,Rebull, L. M.,Giorgini, J. D.,& Elliot, J. L.2004*Astrophy. J. Supp. Ser.* 154, 469

Reach, W. T.2004, *Bull. Amer. Astron. Soc.* 36, 43.04 [abstract]

Rieke, G. H., and 42 colleagues 2004, *Astrophys. J. Supp. Ser.* 154, 25

Stansberry, J. A., *et al.* 2006, *Icarus*, submitted

Stansberry, J. A., and 17 colleagues 2004, *Astrophys. J. Supp. Ser.* 154, 463

Stansberry, J. A.,Cruikshank, D. P.,Grundy, W. G.,Margot, J. L.,Emery, J. P.,Fernández, Y. R.,& Rieke, G. H.2005, *Bull. Amer. Astron. Soc.* 37, 52.05 [abstract]

Sykes, M. V.,& Walker, R. G.1992, *Icarus* 95, 108

van Cleve, J. E., and 11 colleagues and 2 teams 2005, *Bull. Amer. Astron. Soc.* 37, 42.05 [abstract]

Werner, W. M., and 25 colleagues 2004, *Astrophys. J. Supp. Ser.* 154, 1

Woodward, C. E.,Kelley, M. S.,Harker, D. E.,Wooden, D. H.,Reach, W. T.,Gehrz, R. D.,& Spitzer GO Comet Team 2005, *Bull. Amer. Astron. Soc.* 37, 16.16 [abstract]